HHS Public Access

Author manuscript

Cell Metab. Author manuscript; available in PMC 2017 February 09.

Published in final edited form as:

Cell Metab. 2016 February 9; 23(2): 315–323. doi:10.1016/j.cmet.2015.11.003.

PTH/PTHrP Receptor Mediates Cachexia in Models of Kidney Failure and Cancer

Serkan Kir[1], **Hirotaka Komaba**[2], **Ana P. Garcia**[1], **P. Economopoulos Konstantinos**[3], **Liu Wei**[3], **Lanske Beate**[2], **A. Hodin Richard**[3], and **M. Spiegelman Bruce**[1,*]

[1]Department of Cancer Biology, Dana-Farber Cancer Institute, Harvard Medical School, Boston, MA, 02215, USA

[2]Department of Oral Medicine, Infection, and Immunity, Harvard School of Dental Medicine, Boston, MA, 02115, USA

[3]Department of Surgery, Massachusetts General Hospital, Harvard Medical School, Boston, MA, 02114, USA

SUMMARY

Cachexia is a wasting syndrome associated with elevated basal energy expenditure and loss of adipose and muscle tissues. It accompanies many chronic diseases including renal failure and cancer and is an important risk factor for mortality. Our recent work demonstrated that tumor-derived PTHrP drives adipose tissue browning and cachexia. Here, we show that PTH is involved in stimulating a thermogenic gene program in 5/6 nephrectomized mice that suffer from cachexia. Fat-specific knockout of PTHR blocked adipose browning and wasting. Surprisingly, loss of PTHR in fat tissue also preserved muscle mass and improved muscle strength. Similarly, PTHR knockout mice were resistant to cachexia driven by tumors. Our results demonstrate that PTHrP and PTH mediate wasting through a common mechanism involving PTHR and there exists an unexpected crosstalk mechanism between wasting of fat tissue and skeletal muscle. Targeting the PTH/PTHrP pathway may have therapeutic uses in humans with cachexia.

Graphical abstract

[*]Correspondence: bruce_spiegelman@dfci.harvard.edu.

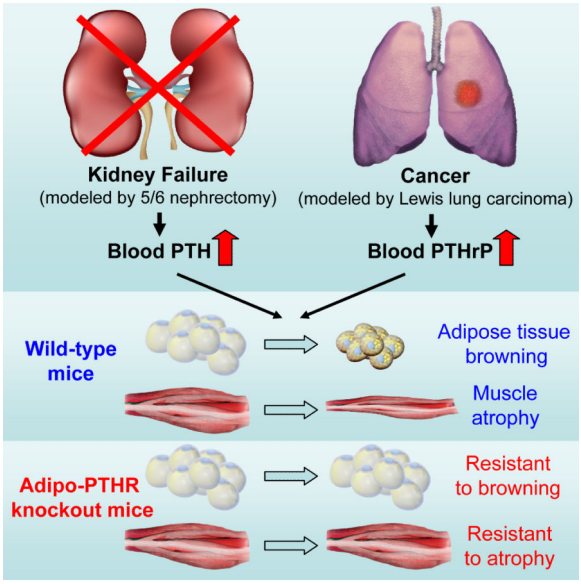

Keywords

Parathyroid hormone (PTH); PTHrP; cachexia; chronic kidney disease; cancer; adipose tissue browning; skeletal muscle atrophy

INTRODUCTION

Cachexia is a wasting syndrome associated with several illnesses including cancer, chronic kidney disease (CKD) and heart failure. Elevated basal energy expenditure in these disorders leads to wasting of adipose tissue and skeletal muscle through enhanced fat and protein catabolism. About half of all cancer patients suffer from cachexia (Argiles et al., 2014). Up to 75% of CKD patients undergoing dialysis therapy has been reported to show signs of wasting (Mak et al., 2011). Cachexia leads to poor outcomes and is an important risk factor for mortality. Cachexia is very different from malnutrition as it cannot be overcome by nutritional supplementation. There are currently few if any effective therapies against cachexia (Fearon et al., 2013; Penna et al., 2010).

There are now known to be at least two types of uncoupling protein 1 (UCP1)-expressing adipocytes (Peirce et al., 2014). Classical brown fat is located mainly in the interscapular region in rodents while pockets of such cells can also be found in white adipose tissues upon cold exposure or with certain hormones. These latter cells come from a distinct cell lineage from classical brown fat and are termed beige adipocytes (Wu et al., 2012). The thermogenic activity of brown/beige fat contributes significantly to energy expenditure in rodents. Both brown and beige fat cells are also found in humans and play a role in energy homeostasis (Cypess et al., 2013; Virtanen et al., 2009). Several studies have described activation of brown fat in rodent models of cancer cachexia; anecdotal reports also show activated brown fat in at least some cachectic patients (Bianchi et al., 1989; Bing et al., 2000; Brooks et al., 1981; Roe et al., 1996; Shellock et al., 1986; Tsoli et al., 2012). Recently, “browning” of the

white fat depots has been shown to drive wasting in rodent models of cancer cachexia (Kir et al., 2014; Petruzzelli et al., 2014; Tsoli et al., 2012).

Our recent study identified parathyroid hormone-related protein (PTHrP), a tumor-derived small polypeptide, as an inducer of thermogenic gene expression and wasting in adipose tissue (Kir et al., 2014). Interestingly, neutralization of PTHrP by a specific antibody attenuated wasting of both fat tissue and skeletal muscle in tumor-bearing mice (Kir et al., 2014). PTHrP is overexpressed by many tumors and its presence in the circulation correlates with a greater degree of wasting in metastatic cancer patients (Kir et al., 2014). PTHrP and parathyroid hormone (PTH) share the same cell surface receptor, PTH/PTHrP receptor or PTHR (Vilardaga et al., 2011). While PTH secreting tumors are very rare, secondary hyperparathyroidism is frequently observed among CKD patients (Bayne and Illidge, 2001; Levin et al., 2007; Tentori et al., 2015). Here, using fat-specific PTHR-deficient mice, we investigated the role of the adipose PTH/PTHrP pathway in cachexia associated with both CKD and cancer. Our results demonstrate that mice lacking PTHR in their fat tissue are resistant to cachexia driven by renal failure and tumors.

RESULTS

5/6 Nephrectomy Causes Adipose Tissue Browning and Cachexia

5/6 Nephrectomy is a common experimental model for kidney failure; this involves removal of one kidney and 2/3 of the other (Deboer, 2009). Nephrectomized mice suffer cachexia and have elevated circulating PTH. We utilized this model to investigate the roles of PTH in CKD-associated cachexia. Nephrectomized mice developed uremia as assessed by blood urea nitrogen (BUN) levels and displayed elevated circulating PTH (Figure 1A, 1B and S1A). These mice showed reduced body weight compared to sham-operated controls (Figure 1C). The weight loss phenotype was accompanied by increased energy expenditure, as shown by elevated O_2 consumption and elevated heat production (Figure 1D and S1B). CO_2 production was also elevated with no changes in respiratory quotient (Figure S1C and S1D). Importantly, the weight loss was not due to increased physical activity or reduced food intake (Figure 1E and S1E). We further documented the cachexia phenotype by measuring weight of fat and skeletal muscle tissues. Epididymal white adipose tissue (eWAT; a visceral fat depot), inguinal white fat (iWAT; a form of subcutaneous fat), interscapular brown fat (iBAT), and gastrocnemius muscle all exhibited significant decreases in total mass (Figure 1F, S2A and S2B). We performed gene expression analysis to understand the mechanisms involved. Expression of the thermogenic genes *Ucp1*, *Dio2*, *Cidea* and *Pgc1a* were induced in iWAT, iBAT and to a lesser extent in eWAT (Figure 1G, 1H, and S2C). Skeletal muscle wasting of the nephrectomized mice was also accompanied by a decrease in expression of the pro-growth hormone *Igf1* and induction of the muscle atrophy-related genes *Murf-1*, *Atrogin-1* and *Myostatin* (Figure 1I).

PTH Stimulates Expression of Thermogenic Genes in Fat Tissues

PTHrP is a potent inducer of thermogenic gene expression (Kir et al., 2014). PTHrP and PTH are similar in that they share sequence homology in their first 34 residues and, in all cases studied to date, act on the same cell surface receptor. The elevation of PTH in the

nephrectomized mice led us to ask whether PTH administration could drive a thermogenic program in adipose cultures and *in vivo*. Like PTHrP(1-34), PTH(1-34) and full length PTH(1-84) stimulated mRNA levels of *Ucp1*, *Dio2* and *Pgc1a* when treated on to primary inguinal fat cells (Figure 2A). Both PTH and PTHrP peptides also stimulated UCP1 protein levels and cellular respiration, including uncoupled respiration, through a mechanism involving the PKA signaling cascade (Kir et al., 2014). Furthermore, PTH administration to mice led to induction of these genes in various fat tissues (Figure 2B, 2C and 2D). Therefore, elevations in circulating PTH may induce thermogenesis in fat.

To test the connection between thermogenic gene expression in adipose tissues and PTH levels in humans, we examined primary hyperparathyroidism (PHPT) patients. Subcutaneous and deep cervical fat samples were collected from patients undergoing parathyroidectomy for PHPT. The control group samples were collected from patients undergoing thyroidectomy for benign pathologies (i.e. Graves' disease, benign goiter and Hurtle-cell neoplasm). Importantly, none of the patients had hyperthyroidism which is known to be involved in thermogenic regulation (Table S1). We first compared subcutaneous and deep cervical fat samples from all patients and tested mRNA levels of some marker genes previously described by a study examining gene expression profiles of these anatomical locations (Cypess et al., 2013). We found that expression of *UCP1* and *LHX8* is elevated in deep cervical fat (Figure 3A) while expression of *LEPTIN* and *SHOX2* is enriched in subcutaneous samples (Figure 3B). We next compared mRNA levels of thermogenic genes in the PHPT and control groups. While expression of these genes in subcutaneous fat does not differ between the two groups (Figure 3C), we observed significant upregulation of *CIDEA* and *PGC1*A and an upward trend for *UCP1* and *DIO2* expression in PHPT deep cervical samples (Figure 3D). The deep cervical fat has been shown to have characteristics of both brown and beige fat with significant thermogenic capacity (Cypess et al., 2013). Therefore, it is likely that upregulation of thermogenesis in such fat depots by PTH may contribute significantly to hypermetabolism.

PTHrP and PTH Signal through PTHR to Induce *Ucp1* Gene Expression

To investigate the role of PTHR in cachexia in the models of kidney failure and cancer, we crossed PTHR-floxed mice (*Pth1r*$^{lox/lox}$) (Kobayashi et al., 2002) with Adiponectin-Cre mice to generate fat cell-specific knockout animals (Adipo-PTHR-KO) (Figure S3). We isolated primary fat cells from these mice and treated them with PTHrP, PTH or norepinephrine. While norepinephrine robustly induced *Ucp1* mRNA expression in the knockout cells, PTHrP and PTH completely failed to upregulate *Ucp1* (Figure 4A). Similarly, PTHrP treatment of the knockout mice did not induce expression of the thermogenic genes in white and brown fat depots (Figure 4B, 4C and 4D). These findings indicate that PTH and PTHrP depend entirely on the well-defined receptor PTHR to drive the thermogenic gene program. Of note, we also tried to generate skeletal muscle-specific PTHR knockout mice using human skeletal alpha (HSA)-Cre driver. To our surprise, we were unable deplete PTHR in skeletal muscle tissue despite obtaining very robust Cre expression. This is in agreement with a previous report demonstrating PTHR localization in Pax7+ satellite cells and CD34+ hematopoietic stem cells but not in the mature myotubes (Kimura and Yoshioka, 2014).

Adipo-PTHR-KO Mice Are Resistant to 5/6 Nephrectomy-driven Cachexia

Next, we examined the contribution of elevated circulating PTH to cachexia associated with 5/6 nephrectomy. We examined metabolic phenotypes of 5/6 nephrectomized fat-specific PTHR knockout mice (Adipo-PTHR-KO) and their Wild-type littermates (WT). Both groups developed similar uremia and secondary hyperparathyroidism upon 5/6 nephrectomy (Figure 5A, 5B and S4A). As shown in Figures 1D and S1B, energy expenditure and heat production of the WT mice significantly increased upon nephrectomy while their physical activity was significantly decreased (Figure 5C, 5D and S4B). Interestingly, nephrectomy-driven hypermetabolism was greatly suppressed in Adipo-PTHR-KO mice while their physical activity was improved (Figure 5C and 5D and S4B). CO_2 production, respiratory quotient and food intake were unchanged among Adipo-PTHR-KO mice (Figure S4C, S4D and S4E). In agreement with the metabolic phenotypes, nephrectomized Adipo-PTHR-KO mice lost weight to a lesser extent compared to the WT nephrectomy group, which exhibited severe cachexia (Figure 5E). Wasting of fat tissue and, surprisingly, wasting of skeletal muscle were improved in the Adipo-PTHR-KO group (Figure 5F).

Histological examination of adipose tissues and skeletal muscle showed that deletion of PTHR in fat tissue prevented fat droplet shrinkage and muscle fibers atrophy observed in the WT nephrectomy group (Figure 6A). PTHR depletion also blocked upregulation of thermogenic genes in fat tissues (Figure 6B, 6C and 6D). In addition to preserving muscle mass, nephrectomized Adipo-PTHR-KO mice also maintained their muscle strength, as evidenced by improved grip strength compared to nephrectomized WT mice (Figure 6E). In accordance, induction of atrophy-related genes *Murf-1*, *Atrogin-1* and *Myostatin* was inhibited in the Adipo-PTHR-KO mice (Figure 6F). These findings suggest existence of a PTH-PTHR signaling axis mediating cachexia in kidney failure and an important crosstalk between fat and skeletal muscle wasting. One possible explanation for this crosstalk is that PTHrP-induced, fat tissue-derived circulating factors may trigger muscle atrophy. Using microarrays, we investigated global gene expression profiles of fat cells treated with PTH or PTHrP. Expression of 13 genes which encode secreted proteins were up-regulated by both PTH and PTHrP (Figure S5). These include the circulating bioactive cytokines IL6, IL33, Cxcl1, Cxcl5 and Cxcl14.

Adipo-PTHR-KO Mice Are Resistant to LLC-tumor-driven Cachexia

Results from the 5/6 nephrectomy study prompted us to examine tumor-driven cachexia in the Adipo-PTHR-KO mice using the Lewis Lung Carcinoma (LLC) model. Remarkably, 16 days after tumor inoculation, mice with PTHR knockout in adipose tissues did not suffer significant weight loss while WT mice displayed evident cachexia (Figure 7A). PTHR depletion in fat tissues attenuated wasting of both adipose tissue and skeletal muscle without changing average tumor mass (Figure 7B and 7C). Histological examination of these tissues showed larger fat droplets and muscle fibers in the tumor-bearing Adipo-PTHR-KO mice (Figure 7D). Similar results were also obtained from Adipo-PTHR-KO mice sacrificed 14 days after tumor inoculation when WT controls were experiencing moderate cachexia (Figure S6). Gene expression analysis on these mice indicated that Adipo-PTHR-KO group is resistant to browning induced by LLC tumors (Figure 7E, 7F and 7G). Muscle function of the knockout mice was also significantly improved as atrophy-related gene expression in

their muscle tissue was significantly suppressed (Figure 7H and 7I). These observations are similar to our published results on PTHrP neutralization by a specific antibody given systemically (Kir et al., 2014), but these new data indicate that cachectic effects of tumor-derived PTHrP are essentially entirely mediated by PTHR expressed in fat tissues.

DISCUSSION

Cachexia is a debilitating disease leading to poor outcomes in cancer and other chronic disorders. There is an urgent need for therapeutics against the wasting syndrome. PTHrP is produced by many tumors and it is often involved in the hypercalcemia of malignancy (Iguchi et al., 2001; Mundy and Edwards, 2008). Our recent work demonstrated that tumor-derived PTHrP drives adipose tissue browning and cachexia in tumor-bearing mice even when it is present at levels not sufficient to increase plasma calcium. PTH and PTHrP share the same receptor specificity and therefore may both be involved in cachexia. Circulating PTH has been reported to be elevated in many chronic diseases, particularly, in CKD (Childs et al., 2012; Dolecek et al., 2003; Jackson et al., 2013; Levin et al., 2007; Visser et al., 2003). Taken together, our new findings describe an important role for PTH in CKD-related cachexia. Like PTHrP, PTH potently stimulates thermogenic gene expression in fat tissue. Importantly and surprisingly, loss of PTHR selectively in fat tissues blocks fat and muscle wasting in both CKD and cancer cachexia models. Since loss of PTHR in fat tissue also improves muscle mass and strength, these data argue that there must be indirect mechanisms (involving PTHR function in fat tissue) through which pathological signals go from fat to skeletal muscle.

Chronic kidney failure is a very complex disease. While malnutrition or various comorbid events may contribute to weight loss in CKD patients, increased energy expenditure in certain CKD patients correlates with increased mortality and cardiovascular disease (Neyra et al., 2003; Wang et al., 2004). Interestingly, dialysis patients with hyperparathyroidism were shown to have increased resting energy expenditure that may be reduced after parathyroidectomy (Cuppari et al., 2004). Increased *Ucp1* expression in brown fat was previously implicated in the weight loss of 5/6 nephrectomized mice (Cheung et al., 2014; Cheung et al., 2007). Our findings support the involvement of adipose tissue thermogenesis in this cachexia model and identify PTH as an important driver of thermogenesis and hypermetabolism. As shown above, PTH treatment potently induces thermogenic genes in fat tissue of mice. Furthermore, primary hyperparathyroidism in humans, although not associated with cachexia, led to increased expression of thermogenic genes in deep cervical fat, which possesses some characteristics of brown/beige fat tissue, including significant thermogenic capacity. Therefore, it is possible that secondary hyperparathyroidism associated with CKD and other chronic diseases in humans may lead to inappropriate thermogenesis and trigger wasting in the presence of other contributing factors. Our findings also showed that the PTH/PTHrP pathway stimulates expression of a number of secreted factors in fat cells. Therefore, this pathway has multiple effects on the fat tissue, which may trigger hypermetabolism and skeletal muscle atrophy. Further studies are needed for establishing a role for these other secreted factors in PTH/PTHrP-driven muscle atrophy.

Finally, our work indicates that the PTH/PTHrP pathway is a generally important player in cachexia and targeting this pathway may be useful in fighting against wasting. In fact, our earlier study showed that neutralization of PTHrP by a specific antibody blocks tumor-driven cachexia (Kir et al., 2014). It will be interesting to test if similar approaches may be beneficial against CKD-driven cachexia. Unlike PTHrP, PTH is also involved in regulation of mineral metabolism. Therefore, therapeutic targeting of PTH or PTHR may be limited by their crucial roles in calcium and phosphate regulation.

EXPERIMENTAL PROCEDURES

Reagents

Synthetic mouse PTHrP(1-34), rat PTH(1-34) and rat PTH(1-84) were purchased from Bachem. Mouse intact PTH (1-84) ELISA assay kit was from ALPCO. Norepinephrine was purchased from Sigma. Total-ERK1/2 antibody (#9102) and anti-Ucp1 (ab10983) were purchased from Cell Signaling and Abcam, respectively.

Animal Studies

All animal experiments were approved by the Institutional Animal Care and Use Committee of the Beth Israel Deaconess Medical Center. In all studies, lean, 6-8-week-old, male, C57BL/6 mice were used. *Pth1r*-floxed mice were a gift from Dr. Henry Kronenberg (MGH) (Kobayashi et al., 2002). *Pth1r*-floxed mice (± Adiponectin-Cre) were maintained on a pure C57BL/6 background. All other mice were obtained from Charles River Laboratories. Mice were maintained in 12 hour light/dark cycles (6am-6pm) at 24°C and fed standard irradiated rodent chow diet. 5 million LLC cells per mouse were injected subcutaneously over the flank. Non-tumor bearing control mice received the vehicle (PBS) only. Mice received subcutaneous injections of PTHrP and PTH peptides and all mice were sacrificed between 4pm-7pm. Plasma was collected into EDTA tubes for the PTH ELISA assay. Heparin tubes were used to collect plasma for Blood Urea Nitrogen (BUN) measurements, which were performed with a Vitros analyzer. Whole-body energy metabolism was evaluated using a Comprehensive Lab Animal Monitoring System (CLAMS, Columbia Instruments). Mice were put into metabolic cages between post-surgery weeks 2 and 3 (and sacrificed at week 5), when the difference in body weight between the sham and 5/6 nephrectomy groups was small. CO_2 and O_2 data were collected every 32 minutes for each mouse and were normalized to total body weight. Data on activity, heat generation and food intake were measured at more frequent intervals. For hematoxylin and eosin staining, tissues were fixed in 10% formalin, embedded in paraffin, and cut into 6 μm sections on slides. Whole body fat composition was determined using an EchoMRI^{TM} analyzer.

5/6 Nephrectomy

This procedure involves removing one kidney and 2/3 of the other kidney. The surgery was performed in two phases. The mouse was first anesthetized with isoflurane (inhaled 1%). An incision was made on the right lateral to the spine. The kidney was freed from the surrounding tissue and then decapsulated to preserve the adrenal gland. The upper and lower poles of the kidney were partially resected, leaving 1/3 of the kidney. Bleeding was

controlled by electrocautery. The abdomen was closed with sutures and wound clips. After one week of recovery, the same preparations were made on the left side as for the right side. The renal blood vessels and ureter were cauterized and the kidney was removed by transecting the vessels and ureter. The incision was closed with sutures and wound clips. Control mice received sham operations, which included kidney decapsulation but not removal. Buprenorphine was used as the analgesic for two days post surgeries.

Grip Strength

Forelimb grip strength was assessed on the same day as sacrifice. Each mouse was allowed to grab a bar attached to a force transducer (Model DFX II; Chatillon) as it was pulled by the tail horizontally away from the bar (Cabe et al., 1978).

Cell Culture

Inguinal stromal-vascular (SV) fractions were obtained from 30-35 days-old male mice by the following procedure. Inguinal fat tissue was dissected, washed with PBS, minced and digested for 45 min at 37°C in PBS containing 10 mM CaCl, 2.4 U/mL dispase II (Roche), and 1.5 U/mL collagenase D (Roche). Digested tissue was filtered through a 100-μm cell strainer and centrifuged at 600g for 5 min to pellet the SV cells. These were then resuspended in adipocyte culture medium (DMEM/F12 plus glutamax (1:1; Invitrogen), pen/strep, and 10% FBS), filtered through a 40-μm cell strainer, centrifuged as above, resuspended in adipocyte culture medium and plated. The SV cells were grown to confluency for differentiation, which was induced by the adipogenic cocktail containing 1 μM dexamethasone, 5 μg/mL insulin, 0.5 μM isobutylmethylxanthine (DMI), and 1 μM rosiglitazone in adipocyte culture medium. 2 days after induction, cells were maintained in adipocyte culture medium containing 5 μg/mL insulin and 1 μM rosiglitazone. Starting at day 6, cells were maintained in adipocyte culture medium only and treated with PTHrP and PTH peptides for 2 hours and harvested at day 8.

RT-qPCR

RNA was extracted from cultured cells or frozen tissue samples using TRIzol (Invitrogen), purified with Qiagen RNeasy minicolumns and reverse transcribed using High Capacity cDNA Reverse Transcription kit (Applied Biosystems). Resulting cDNA was analyzed by qPCR using SYBR® GreenER™ PCR Master Mix (Invitrogen). Reactions were performed in 384-well format using an ABI PRISM® 7900HT instrument (Applied Biosystems). Relative mRNA levels were calculated using the comparative CT method and normalized to *cyclophilin* mRNA. The sequence information of the mouse primer sets were published previously (Kir et al., 2014). Sequence information of human primers is as follows: cyclophilin F: 5′-GGAGATGGCACAGGAGGAA-3′, R: 5′-GCCCGTAGTGCTTCAGTTT-3′; *UCP1* F: 5′-GCAGGGAAAGAAACAGCACCT-3′, R: 5′-ACTTTCACGACCTCTGTGGG-3′; *DIO2* F: 5′-ATGCTGACCTCAGAGGGACT-3′, R: 5′-ATCCTCACCCAATTTCACCTGT-3′; *PGC1A* F: 5′-CCTGCATGAGTGTGTGCTCT-3′, R: 5′-CAGCACACTCGATGTCACTCC-3′; *CIDEA* F: 5′-GGAGCTCATCAGCAAGACTCTG-3′, R: 5′-AACTCTTCTGTGTCCACCACG-3′; *LHX8* F: 5′-ACGTGTGATACAGGTGTGGT-3′, R: 5′-

TAACATGGGTGGAGACAGCC-3′; *LEP* F: 5′-GGAACCCTGTGCGGATTCTT-3′, R: 5′-GGAGGAGACTGACTGCGTG-3′; *SHOX2* F: 5′-AGGCTTTTTGACGAGACCCA-3′, R: 5′-AAACCAAACCTGCACTCGGG-3′.

Microarray

Affymetrix mouse genome 430A v2.0 arrays were used to generate expression profile data which was analyzed using dChip software. The GEO accession number for the microarray dataset is GSE74082.

Western Blotting

Frozen tissues were homogenized in a lysis buffer containing 50 mM Tris (pH 7.4), 500 mM NaCl, 1% NP40, 20% glycerol, 5 mM EDTA and 1 mM PMSF, supplemented with protease and phosphatase inhibitor cocktails (Roche). The homogenates were centrifuged at 13,000 rpm for 10 min and the supernatants were used as whole cell lysates. Protein concentration was determined by Bio-Rad Protein assay and 30 μg of protein lysate was used in each SDS-PAGE run. PVDF membrane was blotted with antibodies in TBS containing 0.05% Tween and 5% BSA. For secondary antibody incubation, TBS-T containing 5% milk was used. ECL western blotting substrates from Pierce were used for visualization of the results.

Human Study

This study was approved by the Human Studies Institutional Review Board of the Massachusetts General Hospital (MGH). Individuals who were planned to undergo neck surgery at MGH were identified by K.P.E. and W.L. and written informed consent was obtained by K.P.E. and W.L. before surgeries. Subcutaneous and deep cervical fat samples were collected from patients undergoing parathyroidectomy for PHPT. The control group samples were collected from patients undergoing thyroidectomy for benign pathologies (i.e. Graves' disease, benign goiter and Hurtle-cell neoplasm). Samples collected included excess fat tissue that was resected as part of the surgical procedure. Thyroid and parathyroid cancer patients were excluded from our cohort. Subjects were not excluded based on gender, ethnicity or other demographics.

Statistical Analysis

Values are expressed as mean ± SEM. Significant analysis was performed using two-tailed, unpaired *t* test for single variables and two-way ANOVA followed by Bonferonni post-tests for multiple variables. Two-way ANOVA with repeated measures was used when analyzing body weight and metabolic data such as VO2, VCO2, physical activity and heat output. Graphpad Prism software was used for ANOVA analysis.

Supplementary Material

Refer to Web version on PubMed Central for supplementary material.

ACKNOWLEDGEMENTS

S.K. is a Robert Black Fellow of the Damon Runyon Cancer Research Foundation (DRG-2153-13). H.K. is a JSPS Postdoctoral Fellow for Research Abroad. This work was supported by grants from the NIH (DK31405) and the JPB Foundation to B.M.S. and NIH grant (DK097105) to B.L.

REFERENCES

Argiles JM, Busquets S, Stemmler B, Lopez-Soriano FJ. Cancer cachexia: understanding the molecular basis. Nat Rev Cancer. 2014; 14:754–762. [PubMed: 25291291]

Bayne MC, Illidge TM. Hypercalcaemia, parathyroid hormone-related protein and malignancy. Clin Oncol (R Coll Radiol). 2001; 13:372–377. [PubMed: 11716233]

Bianchi A, Bruce J, Cooper AL, Childs C, Kohli M, Morris ID, Morris-Jones P, Rothwell NJ. Increased brown adipose tissue activity in children with malignant disease. Horm Metab Res. 1989; 21:640–641. [PubMed: 2591881]

Bing C, Brown M, King P, Collins P, Tisdale MJ, Williams G. Increased gene expression of brown fat uncoupling protein (UCP)1 and skeletal muscle UCP2 and UCP3 in MAC16-induced cancer cachexia. Cancer Res. 2000; 60:2405–2410. [PubMed: 10811117]

Brooks SL, Neville AM, Rothwell NJ, Stock MJ, Wilson S. Sympathetic activation of brown-adipose-tissue thermogenesis in cachexia. Biosci Rep. 1981; 1:509–517. [PubMed: 7295902]

Cabe PA, Tilson HA, Mitchell CL, Dennis R. A simple recording grip strength device. Pharmacol Biochem Behav. 1978; 8:101–102. [PubMed: 625478]

Cheung WW, Ding W, Gunta SS, Gu Y, Tabakman R, Klapper LN, Gertler A, Mak RH. A pegylated leptin antagonist ameliorates CKD-associated cachexia in mice. J Am Soc Nephrol. 2014; 25:119–128. [PubMed: 24115476]

Cheung WW, Kuo HJ, Markison S, Chen C, Foster AC, Marks DL, Mak RH. Peripheral administration of the melanocortin-4 receptor antagonist NBI-12i ameliorates uremia-associated cachexia in mice. J Am Soc Nephrol. 2007; 18:2517–2524. [PubMed: 17687077]

Childs K, Welz T, Samarawickrama A, Post FA. Effects of vitamin D deficiency and combination antiretroviral therapy on bone in HIV-positive patients. AIDS. 2012; 26:253–262. [PubMed: 22112601]

Cuppari L, de Carvalho AB, Avesani CM, Kamimura MA, Dos Santos Lobao RR, Draibe SA. Increased resting energy expenditure in hemodialysis patients with severe hyperparathyroidism. J Am Soc Nephrol. 2004; 15:2933–2939. [PubMed: 15504947]

Cypess AM, White AP, Vernochet C, Schulz TJ, Xue R, Sass CA, Huang TL, Roberts-Toler C, Weiner LS, Sze C, et al. Anatomical localization, gene expression profiling and functional characterization of adult human neck brown fat. Nature medicine. 2013; 19:635–639.

Deboer MD. Animal models of anorexia and cachexia. Expert Opin Drug Discov. 2009; 4:1145–1155. [PubMed: 20160874]

Dolecek R, Tymonova J, Adamkova M, Kadlcik M, Pohlidal A, Zavodna R. Endocrine changes after burns: the bone involvement. Acta Chir Plast. 2003; 45:95–103. [PubMed: 14733253]

Fearon K, Arends J, Baracos V. Understanding the mechanisms and treatment options in cancer cachexia. Nature reviews Clinical oncology. 2013; 10:90–99.

Iguchi H, Onuma E, Sato K, Sato K, Ogata E. Involvement of parathyroid hormone-related protein in experimental cachexia induced by a human lung cancer-derived cell line established from a bone metastasis specimen. International journal of cancer Journal international du cancer. 2001; 94:24–27. [PubMed: 11668474]

Jackson AS, Shrikrishna D, Kelly JL, Kemp SV, Hart N, Moxham J, Polkey MI, Kemp P, Hopkinson NS. Vitamin D and skeletal muscle strength and endurance in COPD. Eur Respir J. 2013; 41:309–316. [PubMed: 22556020]

Kimura S, Yoshioka K. Parathyroid hormone and parathyroid hormone type-1 receptor accelerate myocyte differentiation. Sci Rep. 2014; 4:5066. [PubMed: 24919035]

Kir S, White JP, Kleiner S, Kazak L, Cohen P, Baracos VE, Spiegelman BM. Tumour-derived PTH-related protein triggers adipose tissue browning and cancer cachexia. Nature. 2014; 513:100–104. [PubMed: 25043053]

Kobayashi T, Chung UI, Schipani E, Starbuck M, Karsenty G, Katagiri T, Goad DL, Lanske B, Kronenberg HM. PTHrP and Indian hedgehog control differentiation of growth plate chondrocytes at multiple steps. Development. 2002; 129:2977–2986. [PubMed: 12050144]

Levin A, Bakris GL, Molitch M, Smulders M, Tian J, Williams LA, Andress DL. Prevalence of abnormal serum vitamin D, PTH, calcium, and phosphorus in patients with chronic kidney disease: results of the study to evaluate early kidney disease. Kidney Int. 2007; 71:31–38. [PubMed: 17091124]

Mak RH, Ikizler AT, Kovesdy CP, Raj DS, Stenvinkel P, Kalantar-Zadeh K. Wasting in chronic kidney disease. J Cachexia Sarcopenia Muscle. 2011; 2:9–25. [PubMed: 21475675]

Mundy GR, Edwards JR. PTH-related peptide (PTHrP) in hypercalcemia. J Am Soc Nephrol. 2008; 19:672–675. [PubMed: 18256357]

Neyra R, Chen KY, Sun M, Shyr Y, Hakim RM, Ikizler TA. Increased resting energy expenditure in patients with end-stage renal disease. JPEN J Parenter Enteral Nutr. 2003; 27:36–42. [PubMed: 12549596]

Peirce V, Carobbio S, Vidal-Puig A. The different shades of fat. Nature. 2014; 510:76–83. [PubMed: 24899307]

Penna F, Minero VG, Costamagna D, Bonelli G, Baccino FM, Costelli P. Anti-cytokine strategies for the treatment of cancer-related anorexia and cachexia. Expert opinion on biological therapy. 2010; 10:1241–1250. [PubMed: 20594117]

Petruzzelli M, Schweiger M, Schreiber R, Campos-Olivas R, Tsoli M, Allen J, Swarbrick M, Rose-John S, Rincon M, Robertson G, et al. A switch from white to brown fat increases energy expenditure in cancer-associated cachexia. Cell Metab. 2014; 20:433–447. [PubMed: 25043816]

Roe S, Cooper AL, Morris ID, Rothwell NJ. Mechanisms of cachexia induced by T-cell leukemia in the rat. Metabolism. 1996; 45:645–651. [PubMed: 8622610]

Shellock FG, Riedinger MS, Fishbein MC. Brown adipose tissue in cancer patients: possible cause of cancer-induced cachexia. J Cancer Res Clin Oncol. 1986; 111:82–85. [PubMed: 3949854]

Tentori F, Wang M, Bieber BA, Karaboyas A, Li Y, Jacobson SH, Andreucci VE, Fukagawa M, Frimat L, Mendelssohn DC, et al. Recent changes in therapeutic approaches and association with outcomes among patients with secondary hyperparathyroidism on chronic hemodialysis: the DOPPS study. Clin J Am Soc Nephrol. 2015; 10:98–109. [PubMed: 25516917]

Tsoli M, Moore M, Burg D, Painter A, Taylor R, Lockie SH, Turner N, Warren A, Cooney G, Oldfield B, et al. Activation of thermogenesis in brown adipose tissue and dysregulated lipid metabolism associated with cancer cachexia in mice. Cancer Res. 2012; 72:4372–4382. [PubMed: 22719069]

Vilardaga JP, Romero G, Friedman PA, Gardella TJ. Molecular basis of parathyroid hormone receptor signaling and trafficking: a family B GPCR paradigm. Cellular and molecular life sciences : CMLS. 2011; 68:1–13. [PubMed: 20703892]

Virtanen KA, Lidell ME, Orava J, Heglind M, Westergren R, Niemi T, Taittonen M, Laine J, Savisto NJ, Enerback S, et al. Functional brown adipose tissue in healthy adults. N Engl J Med. 2009; 360:1518–1525. [PubMed: 19357407]

Visser M, Deeg DJ, Lips P. Low vitamin D and high parathyroid hormone levels as determinants of loss of muscle strength and muscle mass (sarcopenia): the Longitudinal Aging Study Amsterdam. J Clin Endocrinol Metab. 2003; 88:5766–5772. [PubMed: 14671166]

Wang AY, Sea MM, Tang N, Sanderson JE, Lui SF, Li PK, Woo J. Resting energy expenditure and subsequent mortality risk in peritoneal dialysis patients. J Am Soc Nephrol. 2004; 15:3134–3143. [PubMed: 15579517]

Wu J, Bostrom P, Sparks LM, Ye L, Choi JH, Giang AH, Khandekar M, Virtanen KA, Nuutila P, Schaart G, et al. Beige adipocytes are a distinct type of thermogenic fat cell in mouse and human. Cell. 2012; 150:366–376. [PubMed: 22796012]

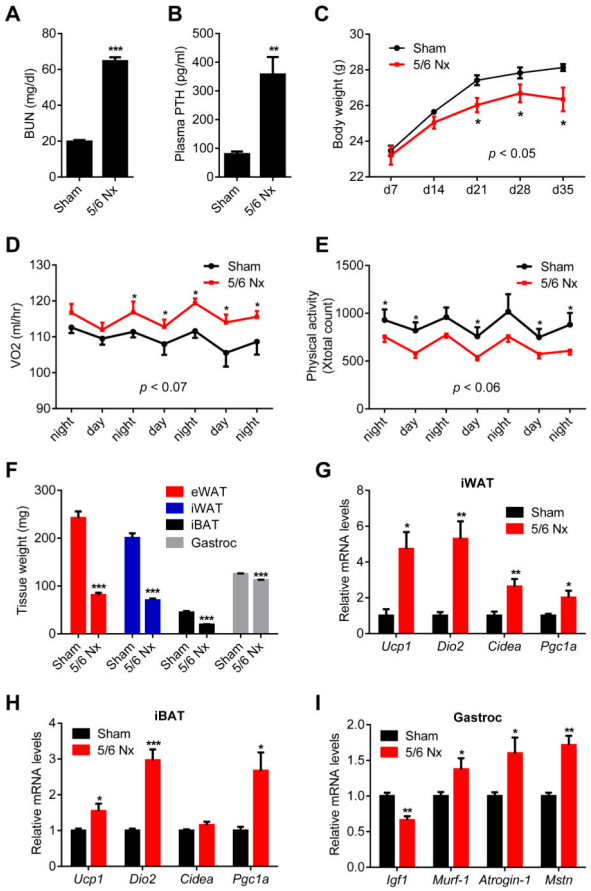

Figure 1. 5/6 nephrectomized mice develop cachexia with adipose tissue browning and skeletal muscle atrophy

(A-I) Mice underwent sham or 5/6 nephrectomy (5/6 Nx) surgery and were sacrificed 5 weeks later (n = 5-7). Blood Urea Nitrogen (BUN) (A), plasma PTH levels (B) and body weight (C) were measured. Mice were placed into metabolic cages between post-surgery weeks 2 and 3, when the difference in body weight was small. Oxygen consumption (VO_2) (D) and physical activity (E) were monitored. Fat and muscle tissues were dissected and weighed (F). mRNA levels in iWAT (G), iBAT (H) and gastrocnemius muscle (I) were determined by RT-qPCR. The values are mean ± SEM. *$P < 0.05$, **$P < 0.005$, ***$P < 0.0005$. See also Figure S1 and S2.

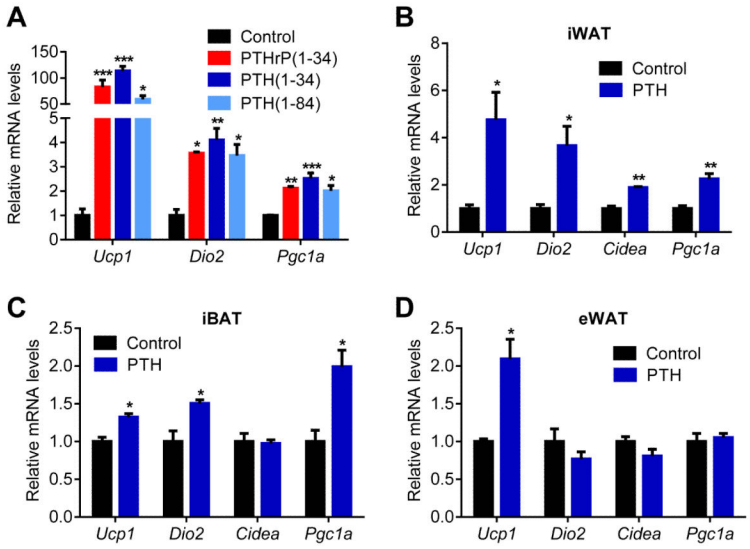

Figure 2. PTH treatment elevates the thermogenic gene program

(A) Primary cultures of inguinal adipocytes were treated with 10 ng/ml PTHrP(1-34), 10 ng/ml PTH(1-34) or 25 ng/ml PTH(1-84) for 2 hr (n = 3).

(B-D) Mice received a single dose of PTH(1-34) (1 mg/kg body weight; SubQ) and were sacrificed 2 hr later (n = 6). Gene expression changes were determined by RT-qPCR. The values are mean ± SEM. **P* < 0.05, ***P* < 0.005, ****P* < 0.0005.

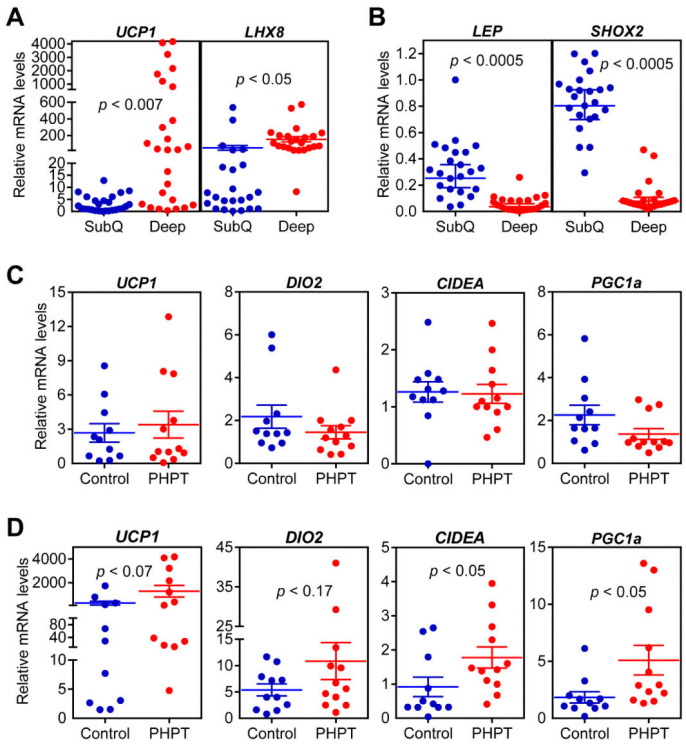

Figure 3. The thermogenic gene program is increased in primary hyperparathyroidism patients

(A-D) Subcutaneous and deep cervical fat samples were collected from patients undergoing neck surgeries. Gene expression levels were compared between subcutaneous and deep cervical samples (n = 23) (A-B) or within subcutaneous fat (C) and deep cervical fat (D) of control and primary hyperparathyroidism patients (PHPT) (n = 11-12). mRNA levels were determined by RT-qPCR. Statistics by two-tailed *t*-test.

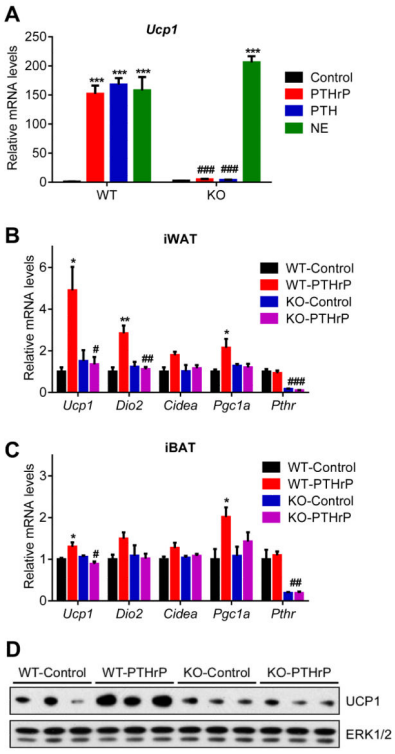

Figure 4. PTH and PTHrP are unable to induce thermogenic genes in the absence of PTHR

(A) Primary adipocytes from wild type and mutant cells were treated with 10 ng/ml PTHrP(1-34), 10 ng/ml PTH(1-34) or 10 nM Norepinephrine (NE) for 2 hr (n = 3). (B-D) Mice received a single dose of PTHrP(1-34) (1 mg/kg body weight; SubQ) and were sacrificed 2 hr later (n = 5-6). Gene expression changes were determined by RT-qPCR. Total UCP1 and ERK1/2 protein levels in inguinal fat tissue were measured by western blotting (D). The values are mean ± SEM. (*) refers to differences compared to the control group. (#) refers to differences between the WT and KO groups. **P* < 0.05, ****P* < 0.0005, ###*P* < 0.0005. See also Figure S3.

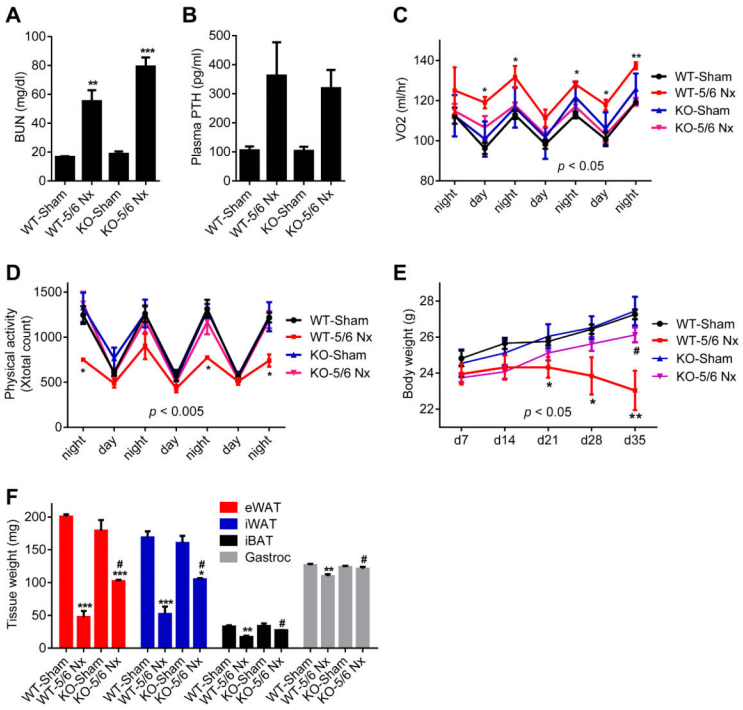

Figure 5. Adipo-PTHR-KO mice are resistant to 5/6 nephrectomy-driven cachexia

(A-F) Mice underwent sham or 5/6 nephrectomy (5/6 Nx) surgery and were sacrificed 5 weeks later (n = 5-6). Blood Urea Nitrogen (BUN) (A) and plasma PTH (B) levels were measured. Mice were placed into metabolic cages between post-surgery weeks 2 and 3, when the difference in body weight was small. Oxygen consumption (VO_2) (C), physical activity (D) and body weight (E) were monitored. Fat and muscle tissues were dissected and weighed (F). The values are mean ± SEM. (*) refers to differences between the Sham and 5/6 Nx groups. (#) refers to differences between the WT-5/6 Nx and KO-5/6 Nx groups. *P < 0.05, **P < 0.005, ***P < 0.0005, #P < 0.05, ##P < 0.005. See also Figure S4.

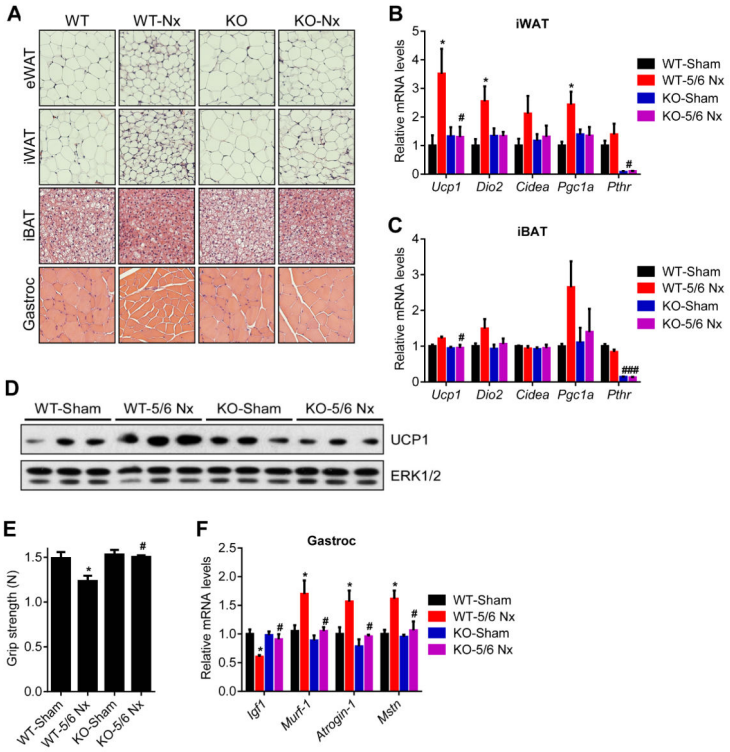

Figure 6. Adipose tissue browning and skeletal muscle atrophy are suppressed in 5/6 nephrectomized Adipo-PTHR-KO mice

(A-F) Mice underwent sham or 5/6 nephrectomy (5/6 Nx) surgery (n = 5-6). H&E staining of adipose tissues and gastrocnemius muscle were shown (A). mRNA levels in iWAT (B), iBAT (C) and gastrocnemius muscle (F) were measured by RT-qPCR. Total UCP1 and ERK1/2 protein levels in inguinal fat tissue were determined by western blotting (D). Muscle function was analyzed by grip strength (E). The values are mean ± SEM. (*) refers to differences between the Sham and 5/6 Nx groups. (#) refers to differences between the WT-5/6 Nx and KO-5/6 Nx groups. *$P < 0.05$, **$P < 0.005$, ***$P < 0.0005$, #$P < 0.05$. See also Figure S5.

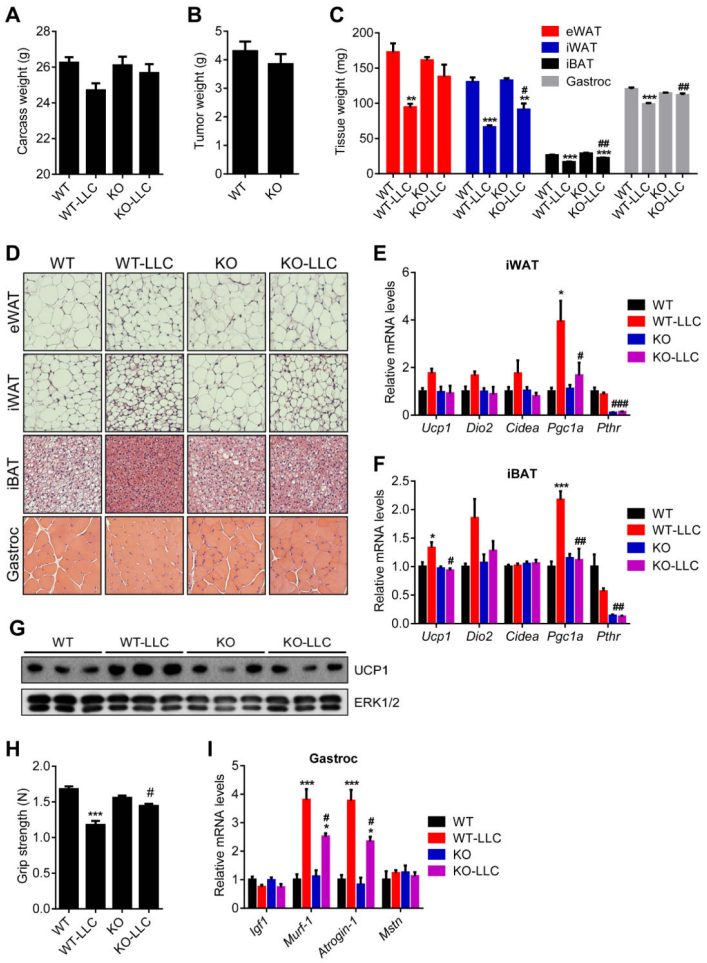

Figure 7. Adipo-PTHR-KO mice are resistant to LLC tumor-driven cachexia

(A-D) Mice inoculated with LLC cells were sacrificed 16 days later (n = 6). Carcass weight (calculated by subtracting tumor weight from the total weight) (A) and tumor weight (B) were shown. Fat and muscle tissues were dissected and weighed (C). H&E staining of adipose tissues and gastrocnemius muscle were shown (D).

(E-G) Mice inoculated with LLC cells were sacrificed 14 days later (n = 4-5). mRNA levels in iWAT (E), iBAT (F) were measured by RT-qPCR. Total UCP1 and ERK1/2 protein levels in inguinal fat tissue were determined by western blotting (G).

(H-I) Mice inoculated with LLC cells were sacrificed 16 days later (n = 6). Muscle function was analyzed by grip strength (G). mRNA levels in gastrocnemius muscle (H) were measured by RT-qPCR. The values are mean ± SEM. (*) refers to differences between the LLC and non-tumor-bearing groups. (#) refers to differences between the WT-LLC and KO-LLC groups. **P* < 0.05, ***P* < 0.005, ****P* < 0.0005, #*P* < 0.05, ##*P* < 0.005, ###*P* < 0.0005. See also Figure S6.